Chapter 3

Chitosan-Clay Based (CS-NaBNT) Biodegradable Nanocomposite Films for Potential Utility in Food and Environment

Asmae Laaraibi, Fatiha Moughaoui, Fouad Damiri, Amine Ouakit, Imane Charhouf, Souad Hamdouch, Abdelhafid Jaafari, Abdelmjid Abourriche, Noureddine Knouzi, Ahmed Bennamara and Mohammed Berrada

Additional information is available at the end of the chapter

http://dx.doi.org/10.5772/intechopen.76498

Abstract

The aim of this work is to design newer material for food packaging applications and to valorize the Moroccan marine wastes using chitosan (CS) prepared from exoskeletons of shrimps. Biodegradable and uniform nanocomposite films developed from sodium bentonite nanoparticles dispersed in chitosan matrix were carefully studied. The montmorillonite is used as nanofiller, and aqueous acetic acid solution is employed as a medium for dissolving and dispersing chitosan and montmorillonite. The existence of dialdehyde chitosan as cross-linking agent was examined. Morphology, thermal behavior, and mechanical properties of the nanocomposite films have been studied using FTIR, TGA, FEGSEM, TEM, XRD, and a tensile test. The XRD results indicate the formation of an intercalated and exfoliated nanostructure at low bentonite content and an intercalated and flocculated nanostructure at high bentonite content. Plastic deformation of the chitosan film is carried out using a thermomechanical treatment in the presence of a solvent and a plasticizer. The nanocomposite films obtained show a good tensile strength due to the reinforcement of chitosan intercalation in the silicate, which is an interesting mechanical property needed for food packaging applications. These nanocomposite films made from naturally occurring materials might play an important role in advanced research in food and environmental science.

Keywords: chitosan, food, environment, montmorillonite, sodium bentonite, films, nanocomposite, biodegradable

IntechOpen

© 2018 The Author(s). Licensee IntechOpen. This chapter is distributed under the terms of the Creative Commons Attribution License (http://creativecommons.org/licenses/by/3.0), which permits unrestricted use, distribution, and reproduction in any medium, provided the original work is properly cited. CC BY

1. Introduction

The increase in living standards, changing consumer habits, and industrial development led to a high consumption of biodegradable plastic materials [1]. One of the best options to reduce current packaging waste is the use of biodegradable films that allow the final replacement of plastic packaging bags which are not recycled and are thus a pollution source. The present research is directed toward the development of biodegradable ecofriendly materials with enhanced properties [2]. Chitosan (CS) is a deacetylated derivative of chitin, which is the most abundant polysaccharide in nature after cellulose; it is a natural polysaccharide, biocompatible, and biodegradable in addition to the antibacterial properties that can be useful in many areas as the food packaging industry. Chitosan which consists of a linear (1–4) linked 2-amino-2-deoxy-D glucan as shown in **Figure 1** is a relatively inexpensive material, next to cellulose.

Chitin and chitosan are biopolymers having immense structural possibilities for chemical and mechanical modifications to generate novel properties, functions, and applications [3, 4], as biomedicine [5, 6], pharmaceuticals [7–9], metal chelation [10, 11], and food additives [12] and in the fabrication of sensors or biosensors [13].

Chitosan is highly soluble in acid aqueous solution. The positive charge and molecular arrangement confer to chitosan's interesting properties [14]. **Figures 2** and **3** illustrate the protonation of chitosan which leads to soluble material. **Figure 4** shows the simulation of protonated chitosan backbone (positive charges of NH^{3+} onto chitosan polymer) in acid aqueous solution. These positive charges cause a mutual repulsion and thus a swelling behavior and good solubility of chitosan. The protonation constants p*K*a of chitosan decrease slightly, from 6.3 when the molecular weight reduces. The degree of deacetylation effects on p*K*a values. The decrease in degree of deacetylation increases the p*K*a. The degree of deacetylation influenced the balance of hydrophobic interactions and hydrogen bondings on chitosan [15].

In the same way, bentonite clays are also abundant and low-cost natural materials. Sodium bentonite is the name for the ore whose major constituent is the mineral, sodium montmorillonite. Montmorillonite is a three-layer mineral consisting of two tetrahedral layers sandwiched around a central octahedral layer. Bentonite is rich in montmorillonite (usually more

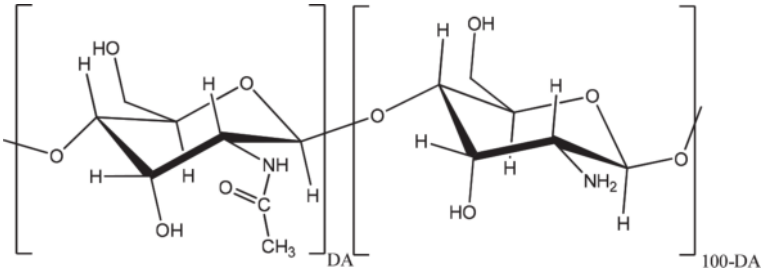

Figure 1. Chemical structure of Chitosan.

http://dx.doi.org/10.5772/intechopen.76498

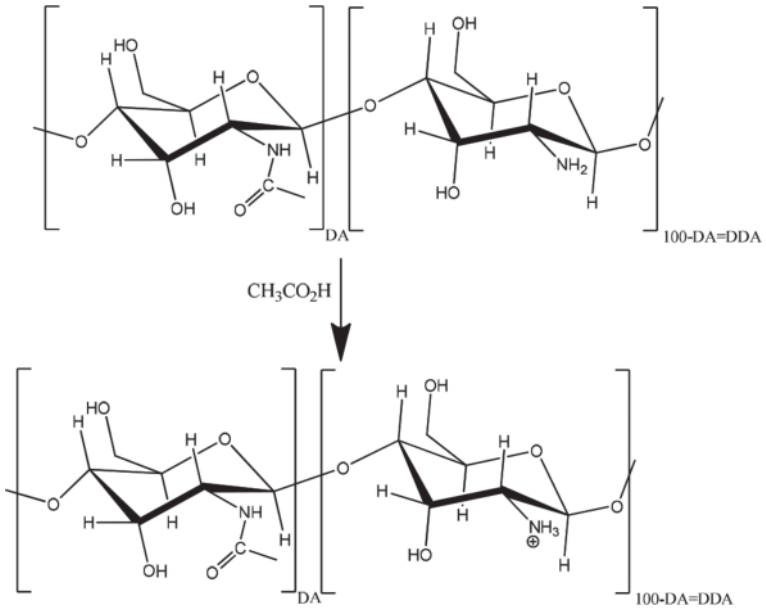

Figure 2. Protonation of chitosan in acetic acid aqueous solution.

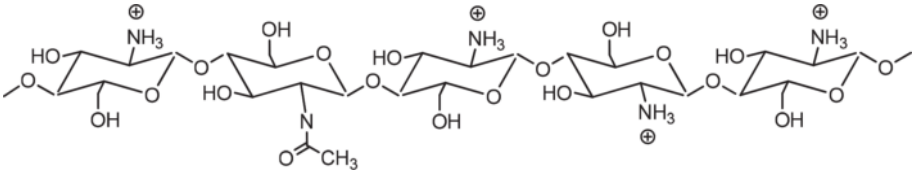

Figure 3. Polymer backbone of protonated chitosan in acid aqueous solution.

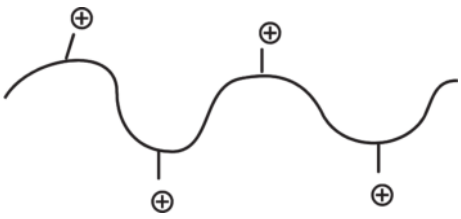

Figure 4. Simulation of protonated chitosan backbone in acid aqueous solution.

than 80%) [16–19]. Bentonite and montmorillonite names are often used interchangeably. However, the terms represent materials with different degrees of purity. Bentonite is the ore that comprises montmorillonite, inessential minerals, and other impurities.

When sodium bentonite comes into contact with water, the atoms and molecules dissolve, and ions with negative charges develop. These negative charges cause a mutual repulsion and thus a swelling within the clay structure. **Figure 5** shows the three-layer structure of a particle of bentonite and its exfoliation in sodium hydroxide aqueous solution.

The cations residing between the layers of sodium bentonite (Na-BNT or simply BNT) are exchangeable with ammonium ions of chitosan. This process converts the hydrophilic surface of the layer into a hydrophobic one, thereby improving the compatibility of nanoclay into polymer matrix.

The three processes that may occur in chitosan polymer and clay mixture, as shown in **Figure 6**, are intercalation, exfoliation, and conventional distribution. Intercalation is a physical process by which a macromolecule like a polymer is inserted in the clay sheets. Such a molecule is flanked by two clay layers and is immobilized and shielded. Exfoliation is a delaminating process wherein the gallery is expanded from its normal size of 1 nm to about 20 nm or higher. Thus there is a clear disruption of the layers which get spatially separated apart bringing about nanoscale dispersion in the polymer matrix. Thus exfoliated clays represent true nanomaterials. Intercalation and exfoliation of the clays can be accomplished using polymer from its solution or a melt [20].

Chitosan/bentonite composites are economically interesting because they are easy to prepare and involve inexpensive chemical reagents. Nanocomposites prepared from chitosan/bentonite shape natural films with a great potential and provide physical protection, they are biocompatible and biologically active toward microbial growth while being nontoxic and biodegradable. These nanobiocomposites obtained by adding nanofillers to biopolymers like chitosan result in very promising materials since they show improved properties with preservation of the material biodegradability without eco-toxicity [21].

Although chitosan/clay nanocomposites are very interesting materials, they were not extensively investigated as potential film packaging for food application. Thus, the aim of this work is to analyze the role of the chitosan/bentonite ratio, the DDA of chitosan, and a plasticizer

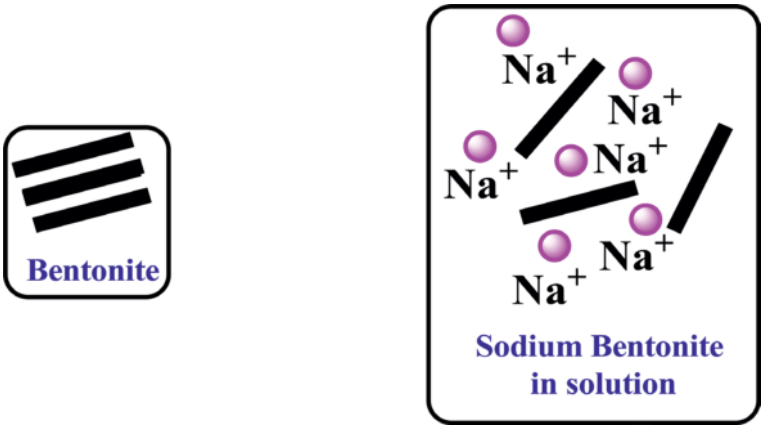

Figure 5. The three sheet structure of a particle of bentonite.

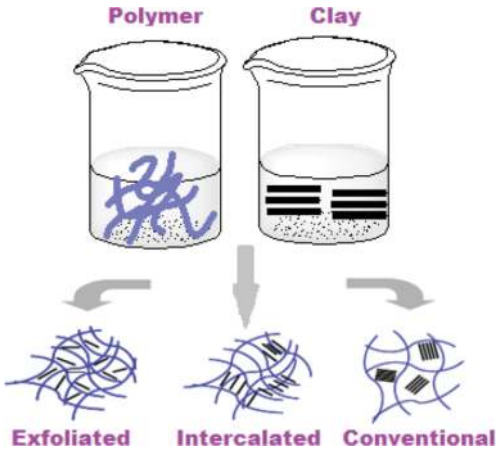

Figure 6. The three processes that may occur in polymer and clay mixture.

specially glycerol in the solution casting process for the achievement of chitosan/clay nanocomposite films. In order to investigate the combined effect of glycerol and unmodified clay on the properties of chitosan-based nanocomposites, films containing different amounts of clay and glycerol were prepared and characterized with particular regard to structural, thermal, and mechanical properties. Finally, new nanocomposite active films were proposed for safe packaging of edibles [22].

2. Material and methods

2.1. Materials

Chitosan (CS) with different degree of deacetylation (DDA) (from 70 to 100%) in powder form was prepared in our laboratory from exoskeletons of shrimp waste and purified [23, 24]. The chitosan chemical structure is schematically shown in **Figure 1**. The degree of deacetylation (DDA %) was determined by conductimetric titration [20].

Analytical grade sodium periodate ACS reagent, 99.8–100% dry basis, and bentonite were purchased from Sigma-Aldrich. Sodium bentonite used in this study was purified according to the method reported by H. Sedighi et al. [25]. The bentonite ore was beneficiated to improve its montmorillonite content by removing the impurities, generally albite, calcite, dolomite, orthoclase cristobalite, and quartz. The crude sample was primarily crushed at the size of 2 mm, and 5 g of bentonite powder was added to 100 mL of hot deionized water and stirred for 2 h. The separation of the impurities is obtained by a sedimentation process of the solution. The settled precipitate is mostly impurities, and the solid collected from the supernatant is generally pure montmorillonite. The slurry and solid phases were separated by filtration, and the remaining solid was dried at 150°C. All the other chemicals used are of analytical grade and used as received.

2.2. Preparation of chitosan film

Chitosan solution was prepared by dissolving 1 g of chitosan powder in 100 ml of aqueous acetic acid solution (1%, v/v), under continuous stirring at room temperature for 2 h followed by vacuum filtering to remove the insoluble residue. This solution was cast into Petri dishes and dried at 50°C for 20 h to evaporate the solvent and form the films. The dried films were soaked with an aqueous solution of 0.05 M NaOH to remove residual acetic acid, followed by rinsing with distilled water to neutralize, and then dried at room temperature.

2.3. Preparation of chitosan/bentonite (CS/Na-BNT) films

Chitosan/Na-BNT (also described as CSBNT) films were prepared using the casting/solvent evaporation technique. Firstly, 1% chitosan solutions were prepared by dissolving 1 g of chitosan powder in 100 ml of aqueous acetic acid solution (1%, v/v), under continuous stirring at room temperature for 2 h followed by vacuum filtering to remove the insoluble residue. Nanocomposite samples were obtained by dispersing selected amounts of bentonite in aqueous solution and stirred at 50°C until swelling was completed. After, the dispersion was slowly added to the CS solution to reach a final clay concentration of 1, 2, 3, and 5 wt% followed by stirring at room temperature for 5 h and then for 30 min at 25°C in ultrasonic bath. The amounts of chitosan, clay, and plasticizer used for each sample are listed in **Table 1**. For example, the composite film CSBNT1% is 1% BNT and 99% CS prepared from 1 g chitosan and 0.0101 g bentonite.

The nanocomposite solutions were then poured into Petri dishes and dried at 50°C for 20 h to evaporate the solvent and form the films. Free chitosan and nanocomposite films plasticized with glycerol were obtained by adding glycerol (30% (wt/wt) on solid CS) to the CS solution while stirring for 20 min at room temperature.

Following the same procedure used for chitosan films, the dried films were soaked with an aqueous solution of 0.05 M NaOH to remove residual acetic acid, followed by rinsing with distilled water to neutralize, and then dried at room temperature.

Chitosan/Na-BNT/cross-linker films were prepared using same method of manufacturing of chitosan/Na-BNT films. The dialdehyde chitosan was used as cross-linker and prepared according to I. Charhouf et al. [26] method and added after dispersing BNT in CS solution.

2.4. Oxidation of chitosan (cross-linker)

2.4.1. Preparation of dialdehyde chitosan

Mix 1 g chitosan ([CS] = 5.34 mM) in suspension with 50 ml HCl (10^{-3} M) (pH ranging from 4 to 5) with magnetic stirring. Mix with 1 ml aqueous solution of sodium periodate 0.534 mM, P0 = 0.1 (P0 = moles of $NaIO_4$ x moles of CS). The reaction was carried out at 4°C in the dark

Sample	Chitosan (g)-wt%	BNT (g)-wt%	Glycerol (g)-wt%
CS	1–100%	—	—
CSBNT1%	1–99%	1%	—
CSBNT2%	1–98%	2%	—
CSBNT3%	1–97%	3%	—
CSBNT5%	1–95%	5%	—
CSG	1–70%	—	30%
CSGBNT1%	1–69%	1%	30%
CSGBNT2%	1–68%	2%	30%
CSGBNT3%	1–67%	3%	30%
CSGBNT5%	1–65%	5%	30%

CS: Chitosan, BNT: bentonite, CSBNT1%: Film chitosan/bentonite 1%, CSBNT2%: Film chitosan/bentonite 2%, CSBNT3%: Film chitosan/bentonite 3%, CSBNT5%: Film chitosan/bentonite 5%, CSG: Film Chitosan/Glycerol, CSGBNT1%: Film Chitosan/Glycerol/bentonite 1%, CSGBNT2%: Film Chitosan/Glycerol/bentonite 2%, CSGBNT3%: Film Chitosan/Glycerol/bentonite 3%, CSGBNT5%: Film Chitosan/Glycerol/bentonite 5%.

Table 1. Amounts (g and wt %) of chitosan (CS), glycerol (G), bentonite (BNT), used for the preparation of chitosan, chitosan/glycerol, chitosan/BNT, and chitosan/glycerol/BNT.

for 30 minutes. After reaction, to eliminate the unreacted periodate, add 1 ml ethylene glycol. The oxidized chitosan was washed by distilled water for 4 h and freeze-dried.

The oxidation of chitosan using NaIO4 was well characterized as reported by I. Charhouf et al. [26]. In this work, we partially oxidized chitosan with a very few amount of sodium periodate. It is clearly seen from **Figure 7** that the oxidation reaction leads to opened structure of chitosan with dialdehyde functions.

2.5. Characterization and measurements

2.5.1. Infrared spectroscopy (FTIR)

Fourier transforms infrared (FTIR) spectra of the chitosan films and the chitosan/clay films were collected using a Tensor 37 FT-IR spectrophotometer (Spectrum 400 Perkin Elmer) operating in the range of 400–4000 cm^{-1} at a resolution of 4 cm^{-1}.

2.5.2. Mechanical properties: tensile measurement

Mechanical properties of chitosan/clay nanocomposite were measured with a Universal Testing Machine Ludwig mpK, tensile strength (TS), and percentage elongation at break (EL) of the films at 25°C according to ASTM D882 standard procedures [27]. The films were cut to a dog bone shape with a rectangular midsection (100 mm long x15 mm wide) flaring to 25 mm x

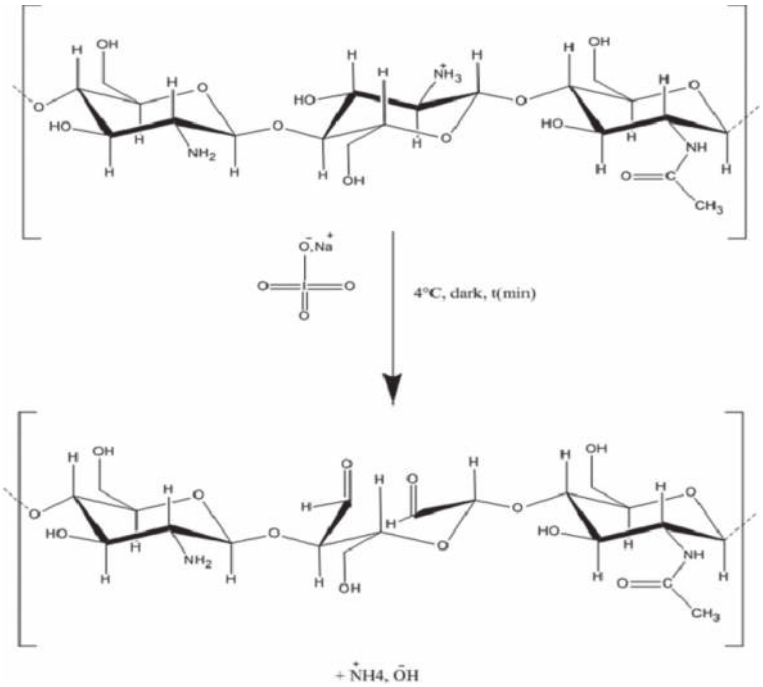

Figure 7. Oxidation reaction of chitosan by sodium periodate.

35 mm sections on each end. The thickness of each sample was measured with micrometer at three different locations and averaged. The films were conditioned at 50% RH for 72 h before each test. A 100 N load cell was used and the extension rate was set at 5 mm/min [28].

The tensile strength (σ) and percentage of elongation at break (E) were calculated using the following equations:

$$\sigma = F_{max}/A. \quad (1)$$

$$E = \Delta l/L_0 \times 100\,\%. \quad (2)$$

where F maxis the maximum load (N), A is the initial cross-sectional area (m^2), Δl is the extension of film strips (m), and L_0 is the initial length (m).

2.5.3. Thermal stability analysis

The thermal properties of nanocomposites and pure chitosan were investigated by thermogravimetric analysis (TGA). Samples were placed in the balance system and heated from 25 to 600°C at a heating rate of 10°C/min under a nitrogen atmosphere. Three replicates were tested for each sample.

http://dx.doi.org/10.5772/intechopen.76498

2.5.4. XRD analysis

The X-ray diffraction analysis of the obtained films was performed by diffractometer with Cu Kα radiation (λ = 1.5418 A°) at room temperature. XRD scans were performed on sodium bentonite, chitosan films, and chitosan/bentonite films with a 2θ range between 5°-30°, at a scanning rate of 1°/min and scanning step of 0.01°.

2.5.5. Morphological analysis

Conventional high-vacuum scanning electron microscopy (SEM) images were also taken to visualize the structure of chitosan and oxidized chitosan. Chitosan and oxidized chitosan were freeze and dried for 24 h and were sprayed on silicon wafer substrate, then sputter-coated with gold (Agar Manual Sputter Coater; Marivac Inc., Montreal, QC, Canada), and imaged using a Quanta 200 FEG Environmental Scanning Electron Microscope (FEI Inc., Hillsboro, OR). Observations were performed at 20 kV using the high-vacuum mode.

The microstructural characterization of nanocomposites was carried out on the following samples: CSBNT3%, chitosan/bentonite 3%; CSBNT5%, chitosan/bentonite 5%; CSBNT10%, chitosan/bentonite 10%; CSBNT20%, chitosan/bentonite 20%; and CSG, chitosan/glycerol. Samples in powder form were coated in epoxy and ultramicrotomed with a diamond knife at -100°C. The recovered thin sections were observed at transmission electron microscope (TEM) (JEOL 2011) operating at 200 kV and the remaining blocks at field emission gun scanning electron microscope (FEGSEM) (Hitachi S 4700) at 1 kV after a slight platinum metal deposition.

3. Results and discussion

3.1. Preparation of bionanocomposite films

The intercalation of the cationic biopolymer chitosan into layered silicate clay (bentonite) through a cation exchange process results in nanocomposites with interesting structural and functional properties. Chitosan/Na-BNT films were prepared using the same method of manufacturing of chitosan films. However, Na-BNT was exfoliated in sodium hydroxide aqueous solution, purified, and washed prior to be added to chitosan solution. Organic matter is present in bentonite as intrinsic impurities composed predominantly of humid substances. Since competitive reactions can take place between the organic matter present in the bentonite and the chitosan, the extent of intercalation and polymer/clay interactions can be affected. Purification capable of removing of organic matter from bentonite before intercalation is fundamental.

The plasticization action of water molecules on hydrocolloid-based films has been widely reported in the literature [29, 31, 32]. In addition to water, the most commonly used plasticizer was glycerol (G), thus nearly systematically incorporated in most of biopolymer films [30]. Glycerol is indeed a highly hygroscopic molecule generally added to film-forming solutions to prevent film brittleness [31, 32]. The interest in use of the glycerol is that it acts as plasticizer and reduces the intermolecular forces by increasing the mobility of the biopolymer chains. The

glycerol reduces the extent interactions between Na-BNT stacks making it possible to achieve a better dispersion of nano-sized filler and can modify the ability of water to swell BNT in the aqueous solution, due to the ability to reduce the surface energy of aqueous solution.

In this study as shown in **Figure 8**, chitosan (CS)/(BNT) nanobiocomposite and chitosan (CS)/(BNT)/cross-linker films were prepared by the intercalation of chitosan in bentonite to form miscible, biodegradable nanocomposite material used as packaging films for food preservation.

Periodate oxidation of chitosan have been relatively little explored, with only a few studies on the periodate oxidation reaction and products formed. Recently, Charhouf et al. [33] studied the periodate oxidation and the physical characterization of oxidized chitosan more in detail. The periodate oxidation of chitosan obviously leads to changes in the chemical structure. The cleavage of C2–C3 in chitosan (CS) units leads to the formation of a dialdehyde. Reaction of cross-linking chitosan and dialdehyde chitosan takes place when dialdehyde group reacts with amine moiety of unmodified chitosan as shown in **Figure 9** giving a cross-linked material.

The nanocomposite films prepared by casting technique using two inexpensive resources available and biocompatible (chitosan and Na-bentonite) were obtained as shown in **Figure 10**.

The presence of a group like hydroxyl, on the surface of chitosan, facilitates encapsulation of essential oils (EOs) or bioactive compound. The nanoemulsions were used to stabilize the EOs in the chitosan matrix, without altering its film-forming properties [34]. We investigated different emulsion formulations to encapsulate essential oils and to study their effects on the in vitro antimicrobial activity against various microorganisms. **Figure 11** shows images of antimicrobial films casted from solutions containing modified chitosan (2% w/w), dyes, and essential oils (0.05% w/w).

Rosemary essential oil, with its warm and penetrating aroma, is one of the most stimulating oils used in aromatherapy. Rosemary was one of the earliest plants to be used in medicine, as well as for cooking. It has a very strong antiseptic action so it is terrific to use in aromatherapy recipes for cleaning. Incorporation of essential oils (EOs) in chitosan films was studied in order to prepare antimicrobial barriers to be applied to food surfaces. Essential oils

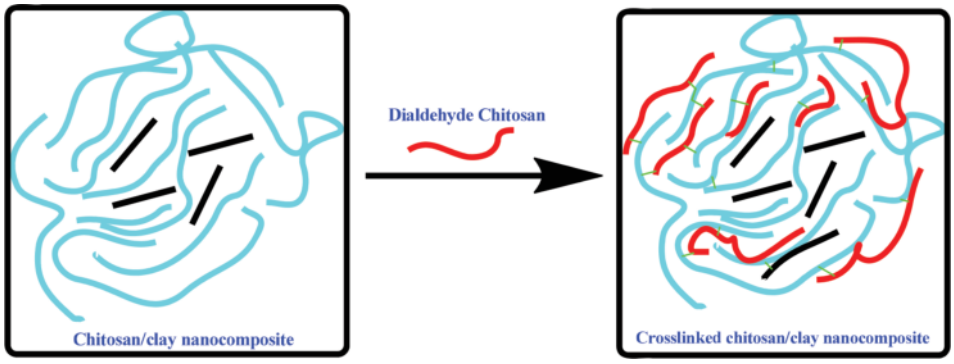

Figure 8. The sheets structure of exfoliated bentonite and dispersed in crosslinked chitosan matrix.

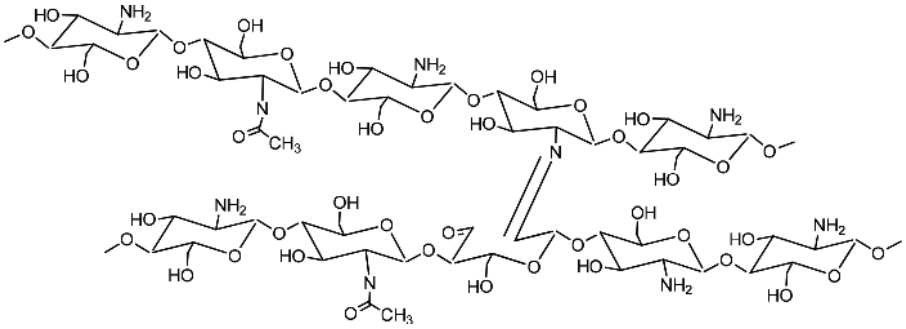

Figure 9. Crosslinking reaction between chitosan and dialdehyde chitosan.

were directly incorporated in the chitosan nanocomposite matrix. The EOs were selected by their ability to develop antimicrobial synergies against *Listeria* bacteria (monocytogenes or innocua) with chitosan, which is characterized by intrinsic antimicrobial properties.

3.2. Infrared spectroscopy (FTIR)

FTIR spectra of chitosan (CS), bentonite (BNT), and chitosan/bentonite nanocomposite (CSBNT) films are displayed in **Figure 12**. The spectrum of chitosan shows a broad peak at 3475.80 cm^{-1} corresponding to amine N–H symmetrical vibration and H bonded O–H group; the peaks at 2924.44 cm^{-1} were assigned to the symmetric and asymmetric $–CH_2$ vibrations of carbohydrate ring. The absorption peak observed at 1618.79 cm^{-1} was assigned to (C = O in amide group, amide I vibration), 1545 cm^{-1} was attributed to ($–NH_2$ bending of amide II), and

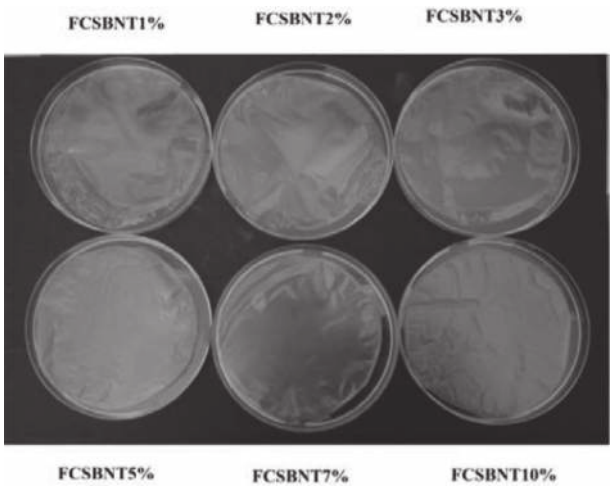

Figure 10. Images of chitosan/bentonite nanocomposite films casted from solutions containing chitosan (2% w/w) and bentonite at various amount of pure clay.

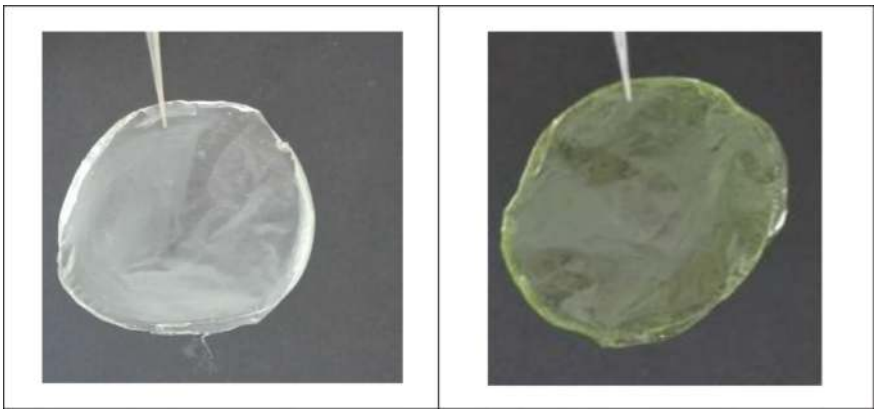

Figure 11. Images of antimicrobial films casted from solutions containing modified chitosan (2% w/w) and essential oils (0.05% w/w) added as pure rosemary essential oil.

1390 cm^{-1} was given to (N–H stretching or C–N bond stretching vibrations, amide III vibration). The peak at 1116.93 cm^{-1} corresponds to the symmetric stretching of C–O–C groups. The absorption peaks in the range 900–1200 cm^{-1} are due to the antisymmetric C–O stretching of saccharide structure of chitosan.

As can be seen in **Figure 12**, the FTIR spectrum of BNT shows a peak at 1010 cm^{-1} that belongs to Si-O-Si linkage. In addition, the characteristic absorption peaks are found at around 3670 cm^{-1} (stretching vibration of Al-OH and OH), at 3465 cm^{-1} (stretching vibration of O-H and H-O-H groups), at 1638 cm^{-1} (H-O-H bending vibration), at 933 cm^{-1} (Al-Al-OH bending frequency), and at 509 cm^{-1} (bending vibration of Si-O).

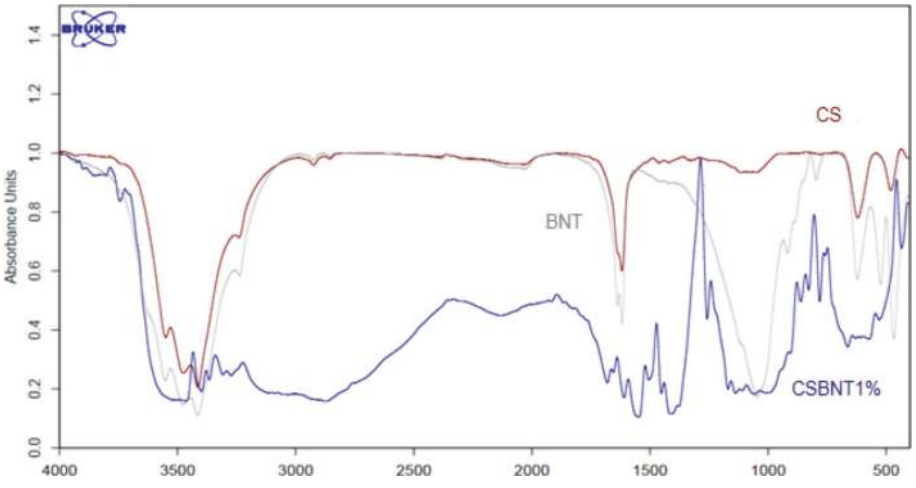

Figure 12. FTIR spectrum of: Chitosan film (FCSBNT0%), Chitosan/BNT films respectively (FCSBNT3%) and (FCSBNT5%).

The FTIR was also used to study the polymer/clay interaction, since a shift in the NH_3^+ vibration may be expected when – NH_3^+ groups interact electrostatically with the negatively charged sites of the clay [35]. Nevertheless, this shift is higher for CSBNT nanocomposite film with the lowest amounts of CS, while the chitosan/clay films with the highest amounts of biopolymer show a frequency value that trends to that observed in the films of pure chitosan (CS). This fact may be related to the $–NH_3^+$ groups that do not interact electrostatically with the clay substrate. The spectrum of CBNT nanocomposite film (**Figure 12**) shows a characteristic band at 3462.78 cm^{-1} attributed to hydrogen bonding formation due to the functional groups of CS (O-H and N-H groups) and BN (O-H groups) [36, 37]. The intensity of the NH_3^+ band also increases for higher amounts of intercalated chitosan. The secondary amide band at 1645 cm^{-1} of chitosan is overlapped with the HOH bending vibration band at 1628 cm^{-1} of the water molecules associated to the chitosan/clay films, which are present as in the starting clay, as expected for a biopolymer with high water retention capability [38, 39].

3.3. Tensile measurements of chitosan (CS), chitosan/bentonite (CSBNT), chitosan/glycerol (CSG), and chitosan/glycerol/bentonite (CSGBNT) films

The stress-strain curves of the tested specimens are being presented in **Figure 13**, while the average values along with the standard deviation of Young's modulus, tensile strength and elongation at break of the films on the stress-strain behavior of the chitosan and chitosan/glycerol films, respectively [40], are shown in **Figure 14**. The higher strength obtained in the case of the CS films can be attributed to more efficient stress transfer between the adjacent chains due to the strong electrostatic interactions between the NH_2 and NH_3^+ groups. The CSG specimen presents almost double strength (at yield and break) and elongation at break. Due to the lower acidity of the diluted films, a weaker hydrogen bond network was established between the amino groups and the glycerol chains. On the other hand, the extensive deformation strengthening in undiluted systems (CSG) suggests the creation of a long-range order and the formation of hydrogen bonding after the addition of glycerol.

The effect of BNT addition on the tensile response of the chitosan and chitosan/glycerol films is being depicted. The stress–strain curves of BNT composite films prepared from the 1 w/v% chitosan solution is being presented. The addition of BNT results in a pronounced enhancement of the stiffness and a dramatic decrease in the elongation at break of all clay-added systems. Further addition of BNT leads in intercalated structures which limited the polymer-clay interactions and thus their reinforcing ability.

The results on mechanical properties showed the increase in the tensile strength (TS) and elastic modulus (EM) of such nanocomposite films can be attributed to the high rigidity and aspect ratio of the nanoclay as well as the high affinity between the chitosan and the bentonite. On the other hand, the CS/BNT nanocomposites have shown significant decrease in elongation at break (EB). This reduction can be attributed to the restricted mobility of macromolecular chains.

In **Figure 14**, effect of BNT addition is being illustrated for the diluted systems (CS nanocomposites). The ductile response of the CS films is maintained after the addition of BNT with strength and a relative lower decrease in the elongation at break. The systems with 3 wt% BNT presented the lowest enhancement in all mechanical properties.

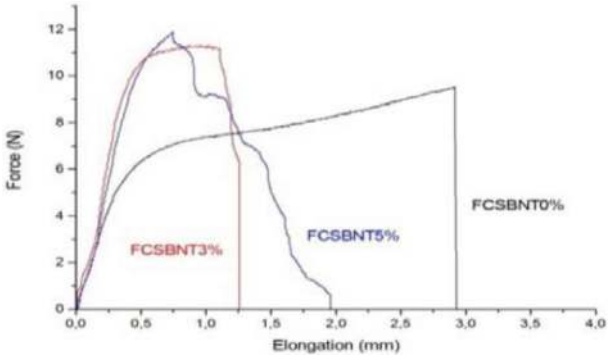

Figure 13. Stress-strain curves of chitosan film (FCSBNT0%), chitosan/BNT films (FCSBNT3%), (FCSBNT5%), respectively.

Figures 13 and **14** present the combined effect of glycerol and BNT on the tensile response of the CS-based nanocomposites. The first observation is that the addition of BNT results in a direct reduction of the strength of the chitosan/glycerol. A completely different stress–strain behavior is being obtained after the addition of BNT in diluted chitosan/glycerol systems (**Figure 14**). The CS/glycerol-based nanocomposites behave like hyperelastic materials rather than like ductile polymers. It is assumed that more water and glycerol are distributed in the chitosan network, inducing a very obvious plasticization effect. The extent of hydrated chitosan crystals was confirmed from the intensities of the XRD patterns. It is very interesting to note that although the mechanical properties of the unreinforced chitosan are comparable before and after the application of the reflux processing, reflux resulted in a fourfold increase of the stiffness and strength of the nanocomposite films.

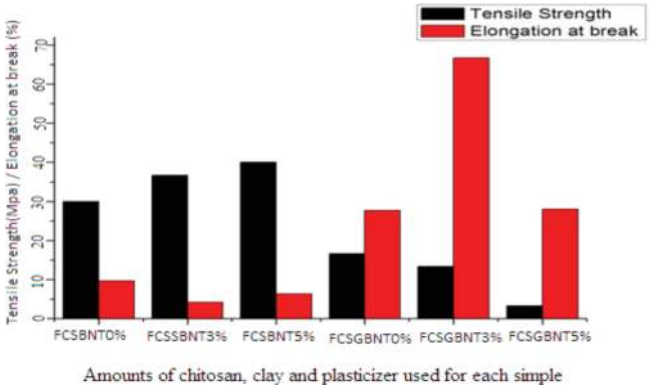

Figure 14. Mechanical properties of chitosan/BNT particles films. Chitosan film (FCSBNT0%), chitosan/BNT films (FCSBNT3%), (FCSBNT5%), respectively, and chitosan/glycerol film (FCSGBNT0%), chitosan/glycerol/BNT films (FCSGBNT3%), (FCSGBNT5%), respectively.

3.4. Thermal stability analysis

The thermal stability of the chitosan (CS) and its nanocomposites has been investigated by TGA under nitrogen (**Figure 15**). There are two steps of degradation. The first range (50–200°C) is associated with the loss of water, whereas the second range at 270°C corresponds to the deacetylation and degradation of chitosan, and the third step, in the temperature range 450–550°C, can be associated with the oxidative degradation of the carbonaceous residue formed during the second step.

The nano-dispersed clay in the chitosan matrix exhibits a significant delay in weight loss. The nanocomposite forms char with a multilayered carbonaceous-silicate structure, which may keep its multilayered structure in the polymer matrix. This high-performance carbonaceous-silicate char builds up on the surface during burning, thus insulating the underlying material and slowing the escape of the volatile products generated during decomposition. The decomposition temperature CS/BNT nanocomposites show higher thermal stability than those of the pure CS. The thermal stability of the nanocomposites increases systematically with increasing clay.

For nanocomposites containing glycerol, a further degradation step at T≈250°C is observed, related to the loss of unbound glycerol, as indicated in **Figure 16**. Furthermore, it can also be observed that the presence of glycerol plasticizer increases of about 20°C the degradation temperature for the third step, irrespective of the presence or not of the clay.

3.5. XRD analysis

The XRD patterns of chitosan and chitosan-based nanocomposite films in the range of 5–30° are shown in (**Figure 17**). The basal plane of BNT shows a reflection peak at about 2θ = 8.8°. After incorporating BNT within CS, with CS/BNT, the basal plane of BNT at 2θ = 8.8° disappears, substituted by a new weakened broad peak at around 2θ = 12.8°–13.0° (CSBNT3%, CSBNT5%). It is suggested that the BNT form intercalated and flocculated structures.

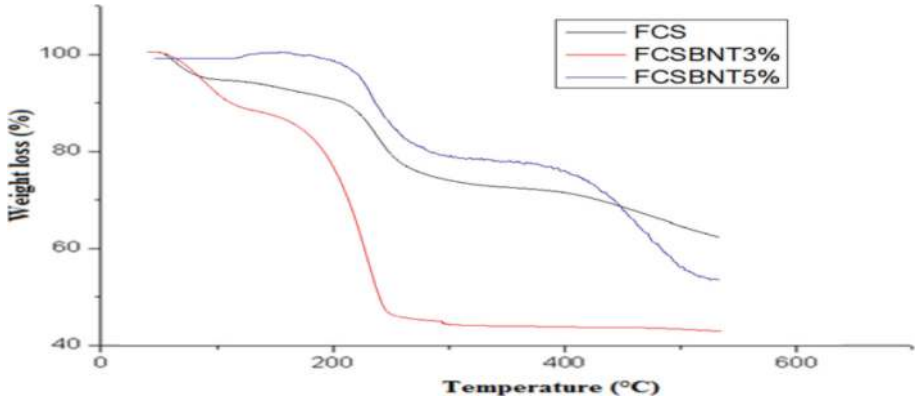

Figure 15. Thermal properties of: Chitosan (FCSBNT0%) and Chitosan/Bentonite films (FCSBNT3%), (FCSBNT5%).

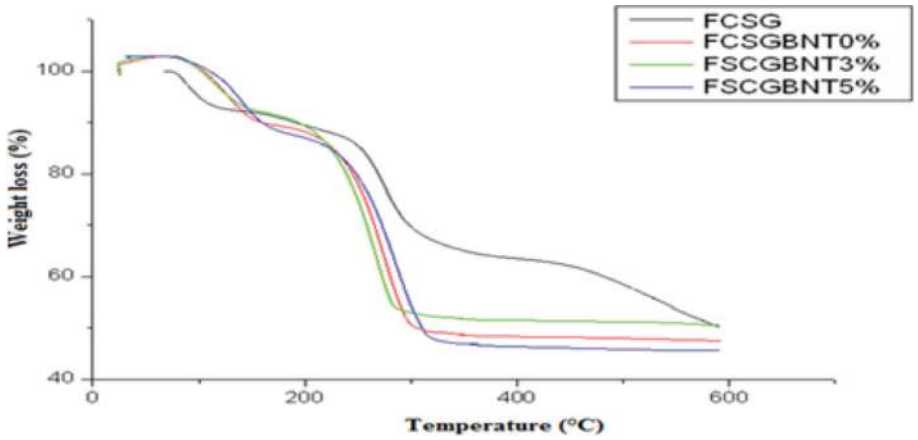

Figure 16. Thermal properties of: Chitosan/Glycerol (FCSG), Chitosan/Glycerol (FCSGBNT0%) and Chitosan/Glycerol/ Bentonite (FCSGBNT3%) and (FCSGBNT5%) films.

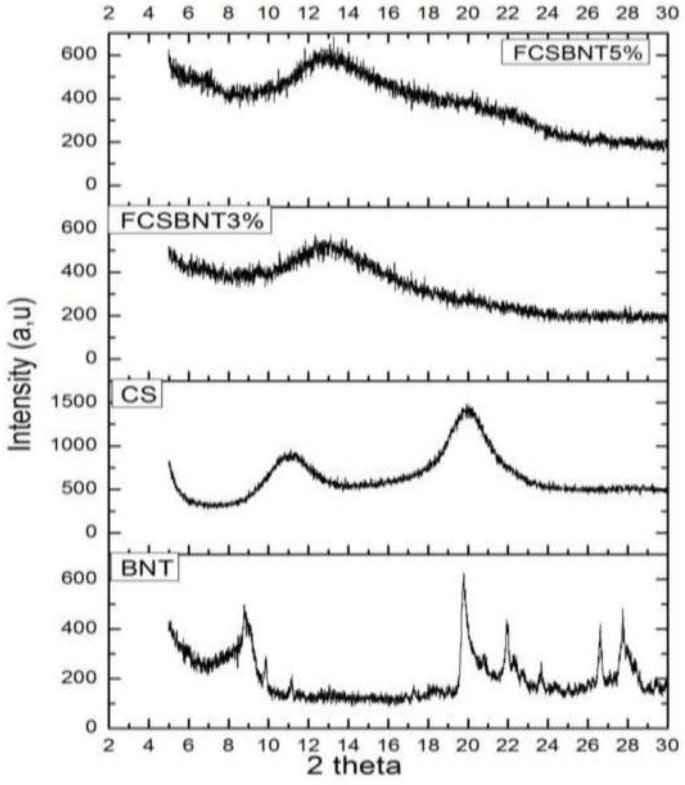

Figure 17. XRD patterns of: Chitosan (CS), Bentonite (BNT) and Chitosan/Bentonite films (FCSBNT3%) and (FCSBNT5%).

On the base of XRD patterns, it is suggested that the BNT forms intercalated and exfoliated structures at higher CS content (CSBNT5%), while decreasing the CS content (CSBNT3%), clay layers (BNT) form intercalated and flocculated structures. According to [23], the formation of flocculated structure in CS/clay nanocomposites can be due to the hydroxylated edge-edge interactions of the clay layers. Since one chitosan unit possesses one amino and two hydroxyl functional groups, these groups can form hydrogen bonds with the clay hydroxyl edge groups. This strong interaction is believed to be the main driving force for the assembly of BNT in the CS matrix to form flocculated structures.

The XRD patterns of chitosan/glycerol films obtained from 30 w/v% solutions are shown in **Figure 18**. The addition of glycerol results in a pronounced peak at 12.5°. Because of the hydrophilic and polycationic nature of chitosan in acidic media, this biopolymer has good miscibility which is attributed to the interaction of glycerol molecules with chitosan

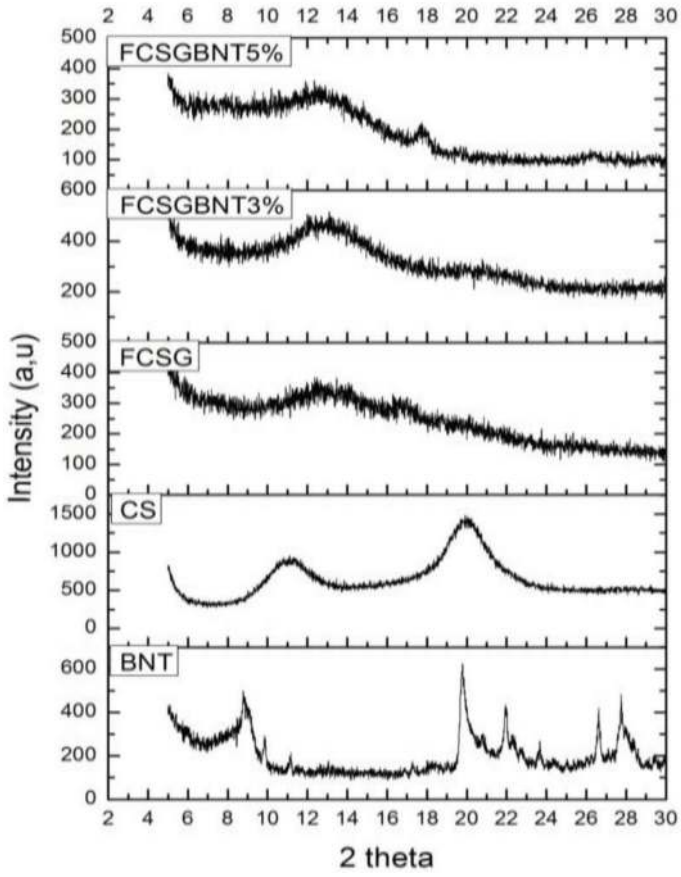

Figure 18. XRD patterns of: Chitosan (CS), Bentonite (BNT), Chitosan/Glycerol (FCSG) and Chitosan/Glycerol/Bentonite films (FCSGBNT3%) and (FCSGBNT5%).

macromolecules. Glycerol favors the chains mobility and thus the chitosan crystallization process in the early stage of the post-processing aging the effect of glycerol addition. The XRD patterns of chitosan/glycerol/BNT films obtained from chitosan solution are shown in **Figure 18**. The combined addition of glycerol and clays resulted in great enhancement of the chitosan crystallinity of the nanocomposite films prepared with 1 w/v% chitosan solution. This indicates that the presence of clay facilitates the distribution of glycerol within the chitosan matrix and the interaction of glycerol molecules with chitosan macromolecules. The combined addition of glycerol and clay had an opposite effect in films obtained from low content chitosan solution leading to decrease of the XRD peaks intensities. In addition a new peak at 18.2° appeared in XRD patterns of all obtained films. This diffraction peak is characteristic for chitosan films prepared using acetic acid solution as solvent.

The addition of glycerol favors the opening of the clay galleries resulting in intercalated nanocomposites in comparison to samples without glycerol.

Chitosan/Na-BNT nanocomposites exhibit an intercalated or intercalated/orientated structure of clays. In particular, the X-ray diffraction results show that in film without glycerol, the BNT stacks lay with their platelet surface parallel to the casting surface. The presence of glycerol, on the other hand, enhances the chitosan intercalation in the silicate galleries and hinders the flocculation process, leaving the BNT stacks randomly orientated in the space.

3.6. SEM and MET images of chitosan, oxidized chitosan, and bionanocomposite materials

The SEM images of chitosan and oxidized chitosan at high vacuum and at different magnifications are shown in **Figure 19**, showing that there is no change of elongated and fibrous network of chitosan, but on the surface of oxidized chitosan, we can see a slight degradation of some leaves.

3.6.1. FEGSEM analysis

We present in this study the microstructural characterization results obtained on the chitosan/Na-BNT nanocomposites too. The dispersion and the exfoliation of the clay were observed at field emission gun scanning electron microscope (FEGSEM) and transmission electron microscopy (TEM).

The results of the observation of the microtome block of chitosan/bentonite (CSBNT3%) and (CSBNT5%) samples are presented in **Figure 20**.

At low magnification, the CSBNT 3% powders were observed, and clusters were found grouped into in the epoxy more matte and dark appearance (**Figure 20a**). Decohesion between the epoxy and the sample powders is visible in greater or lesser proportion, probably due to preparation and cutting. At higher magnification, small clay particles of a few hundred nanometers are observed, which are relatively well dispersed in the polysaccharide (**Figure 20b**). However, a large clay aggregate of about 10 microns was also observed (**Figure 20c** and **d**).

http://dx.doi.org/10.5772/intechopen.76498

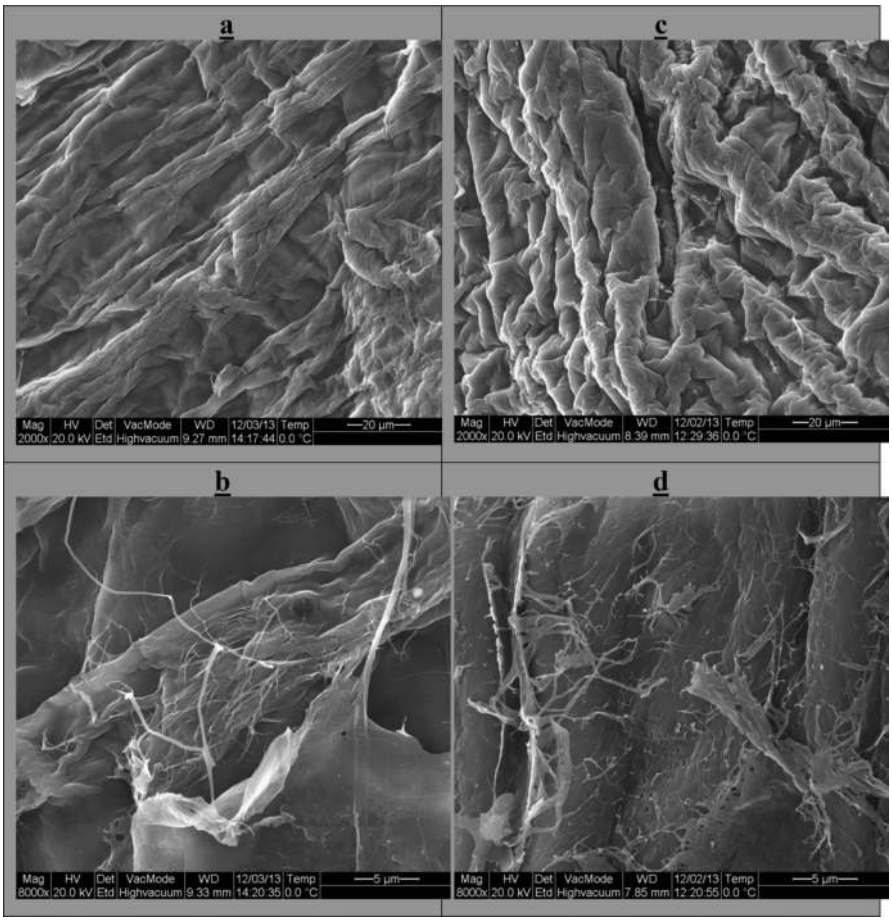

Figure 19. SEM images of (a & b) chitosan and (c & d) oxidized chitosan at different magnifications.

At higher magnification, small clay particles similar in size to those observed in the CSBNT 3% sample are regularly observed with chitosan/BNT 5% as shown in **Figure 21**.

3.6.2. TEM analysis

Transmission electron microscopy (TEM) images indicated that the silicate layers were dispersed in the chitosan matrix. The results of the TEM observation of the chitosan/BNT 3% sample show that small particles of clay from less than 100 nanometers to a few hundred nanometers are observed at low magnification which is consistent with the FEGSEM observations. Larger aggregates of clay are also observed but more rarely.

Depending on the level of the clay particles, the leaflets are sometimes well aligned (**Figure 22**) and sometimes of more unstructured appearance (**Figure 23**). This unstructured aspect of the

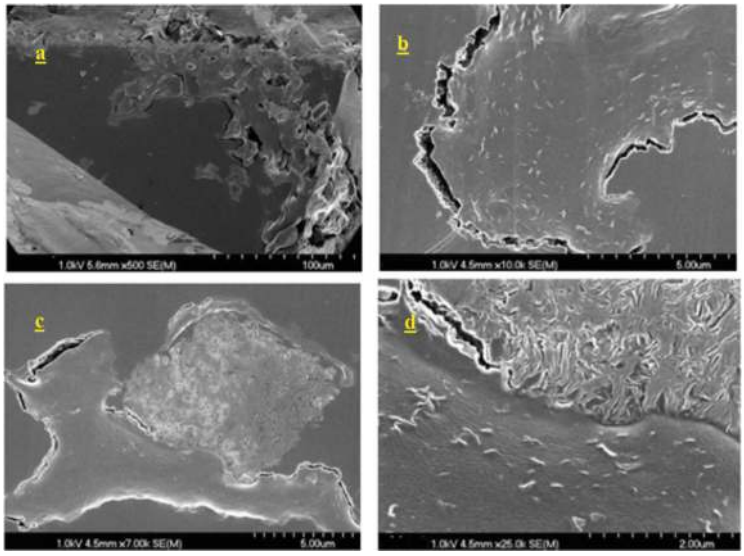

Figure 20. Images of FEGSEM of chitosan/BNT 3%.

clay sheets may be a sign of a more advanced level of intercalation. There are also some isolated single or double leaflets around other clay particles (**Figure 23**), which is a clear sign of exfoliation.

As expected, the concentration of clay in the polysaccharide affects the dispersion of the clay. The higher the concentration, the poorer the dispersion is obtained which is the effect of the greater aggregation of the clay. A good but not always uniform dispersion is observed in chitosan/BNT 3% and 5%. Similarly, the concentration of clay also appears to affect the level

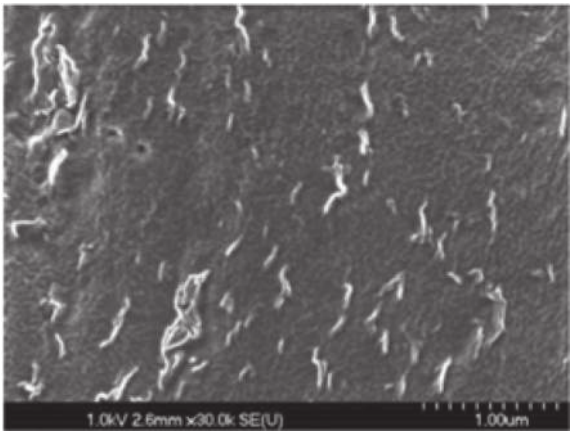

Figure 21. Image of FEGSEM of chitosan/BNT 5%.

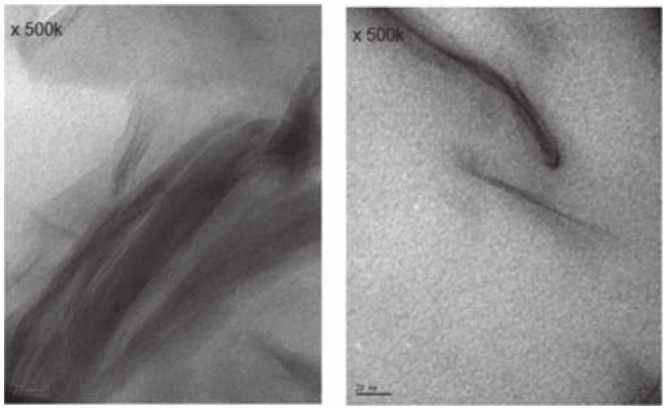

Figure 22. Images TEM of chitosan/BNT 3% (x 500K).

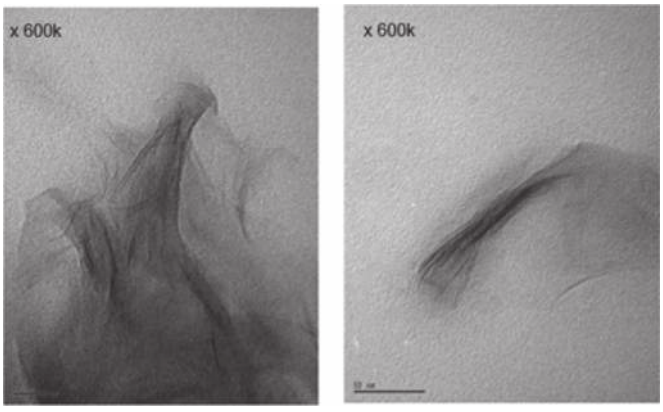

Figure 23. Images TEM of chitosan/BNT 3% (x 600K).

of intercalation/exfoliation. Based on MET observations, signs of exfoliation (the presence of isolated single or double clay leaflets and more unstructured appearance of the leaflets in the particles) are visible in samples of lower clay concentration less than 10%.

4. Conclusion

Natural biopolymer-based biodegradable packaging materials are a new generation of polymers emerging on the packaging market, and driven by the perception that biodegradable plastics are "environmentally friendly," their use is predicted to increase chitosan, a natural material that has interesting antimicrobial and film-forming activities. Its application in films can contribute to food preservation and shelf-life extension. In this study, various films were successfully prepared

by the solution casting technique and characterized with particular regard to structural, thermal, and mechanical properties. Films of chitosan/bentonite, chitosan/glycerol/bentonite, and chitosan/glycerol/bentonite/essential oil nanocomposites were prepared with purified bentonite (BNT), and according to the process used, they might be less expensive than other packaging materials.

Exfoliated chitosan/clay nanocomposites of varying clay contents have been successfully prepared with or without the presence of glycerol (plasticizer) and oxidized chitosan (crosslinker). This approach represents a new route to prepare high-performance nanocomposite materials. The oxidized chitosan could partially react with the amine groups on chitosan; as a result, high mechanical properties can be obtained. The Na-BNT layers are exfoliated by chitosan chains and disorderly dispersed in the chitosan matrix, as confirmed by XRD and TEM characterization. The incorporation of a small amount of clay into the chitosan matrix results in obvious enhancement in the thermal properties of chitosan. The chitosan/clay nanocomposites retain good mechanical properties. Once the clay is exfoliated and efficiently dispersed into the chitosan matrix, the storage modulus and tensile property of the chitosan/clay nanocomposites are significantly improved with respect to that of neat chitosan.

Acknowledgements

This work would not have been possible without the great support of Julian Zhu, a polymer chemist professor at Montreal University, Department of chemistry, Quebec, Canada. This work was supported by the Francophone University Association (AUF).

Author details

Asmae Laaraibi[1]*, Fatiha Moughaoui[1], Fouad Damiri[1], Amine Ouakit[1], Imane Charhouf[1], Souad Hamdouch[1], Abdelhafid Jaafari[2], Abdelmjid Abourriche[1], Noureddine Knouzi[1], Ahmed Bennamara[1] and Mohammed Berrada[1]

*Address all correspondence to: berrada_moh@hotmail.com

1 Department of Chemistry, Laboratory of Biomolecules and Organic Synthesis (BIOSYNTHO), Faculty of Sciences Ben M'Sik, University Hassan II of Casablanca, Morocco

2 Department of Chemistry, Laboratory of Applied Chemistry and environment, Faculty of Sciences and Technologies, University Hassan I of Settat, Morocco

References

[1] Martinho G, Balaia N, Pires A. The portuguese plastic carrier bag tax: the effects on consumers' behavior. Waste Management. 2017;**61**:3-12

[2] Tan W, Zhang Y, Szeto Y, Liao L. A novel method to prepare chitosan/montmorillonite nanocomposites in the presence of hydroxy-aluminum oligomeric cations. Journal of Computer Science and Technology. 2008;**68**:2917-2921

[3] Christensen B, Vold I, Vårum KM. Vårum, chain stiffness and extension of chitosans and periodate oxidized chitosans studied by size-exclusion chromatography combined with light scattering and viscosity detectors. Journal of Carbohydrate Polymers. 2008;**74**:559-565

[4] Mourya VK, Inamdar NN. Chitosan-modifications and applications: opportunities galore. Reactive & Functional Polymers. 2008;**68**:1013-1051

[5] Luo H, Li J, Chen X. Antitumor effect of N-succinyl-chitosan nanoparticles on K562 cells. Biomedicine & Pharmacotherapy. 2010;**64**:521-526

[6] Drumright R, Siegwart DJ, Matyjaszewski K. The development of microgels/nanogels for drug delivery applications. Progress in Polymer Science. 2008;**33**:448-477

[7] Baldrick P. The safety of chitosan as a pharmaceutical excipient. Regulatory Toxicology and Pharmacology. 2010;**56**:290-299

[8] Muzzarelli RA. Genipin-crosslinked chitosan hydrogels as biomedical and pharmaceutical aids. Carbohydrate Polymers. 2009;**77**:1-9

[9] Sinha V, Singla A, Wadhawan S, Kaushik R, Kumria R, Bansal K, Dhawan S. Chitosan microspheres as a potential carrier for drugs. International Journal of Pharmaceutics. 2004;**274**:1-33

[10] Feng Y, Yang L, Li F. A novel sensing platform based on periodate-oxidized chitosan. Analytical Methods. 2010;**2**

[11] Kofuji K, Qian C, Nishimura M, Sugiyama I, Murata Y, Kawashima S. Relationship between physicochemical characteristics and functional properties of chitosan. European Polymer Journal. 2005;**41**:2784-2791

[12] Ferraro V, Cruz I, Jorge RF, Malcata FX, Pintado ME, Castro PML. Valorisation of natural extracts from marine source focused on marine by-products: a review. Food Research International. 2010;**43**:2221-2233

[13] Jerónimo P, Araújo AN, Montenegro M. Development of a sol–gel optical sensor for analysis of zinc in pharmaceuticals. Sensors and Actuators B: Chemical. 2004;**103**: 169-177

[14] Bhuvaneshwari S, Sruthi D, Sivasubramanian V, Niranjana K, Sugunabai J. Development and characterization of chitosan film. Journal of Engineering Research and Applications. 2011;**1**:292-299

[15] Wang QZ, Chen XG, Liu N, Wang SX, Liu CS, Meng XH, Liu CG. Protonation constants of chitosan with different molecular weight and degree of deacetylation. Carbohydrate Polymers. 2006;**65**:194-201

[16] Holzer L, Münch B, Rizzi M, Wep R, Marschall P, Graule T. 3D-microstructure analysis of hydrated bentonite with cryo-stabilized pore water. Journal Applied Clay Science. 2010;**47**:330-342

[17] Li Q, Yue QY, Sun H, Su Y, Gao Y. Comparative study on the properties, mechanisms and process designs for the adsorption of non-ionic or anionic dyes onto cationic-polymer/bentonite. Journal of Environmental Management. 2010;**91**:1601-1611

[18] Utracki L. Clay-containing polymeric nanocomposites. Shrewsbury: Rapra Technology Ltd; Polymer International. May 2005;**54**:860

[19] Wei J, Zhu R, Zhu J. Simultaneous sorption of crystal violet and 2-naphthol to bentonite with different CECs. Journal of Hazardous Materials. 2013;**166**:195-199

[20] Nguyen QT, Baird DG. An improved technique for exfoliating and dispersing nanoclay particles into polymer matrices using supercritical carbon dioxide. Polymer. 2007;**48**:6923-6933

[21] Pillai SK, Ray S. Chitosan-based nanocomposites. Journal of Natural Polymers. 2012:33-68

[22] DeLeo C, Augusto C, do Carmo Goncalves PM, Velankar S. Preparation and characterization of clay nanocomposites of plasticized starch and polypropylene polymer blends. Journal of Polymers and the Environment. 2011;**19**:689-697

[23] Charhouf I. Thesis titled Synthesis and characterization of hydrogel of Chitosan for medical applications. Hassan II University of Casablanca, Faculty of Science Ben M'Sik; 10 January 2015

[24] Lavertu M, Xia Z, Serreqi AN, Berrada M, Rodrigues A, Wang D, Buschmann MD, Ajay Gupta. A validated 1H NMR method for the determination of the degree of deacetylation of chitosan. Journal of Pharmaceutical and Biomedical Analysis. 2003;**32**:1149-1158

[25] Sedighi H, Irannajad M, Gharabaghi M, Amirkabir. Silica impurities removal on bentonite sample for nanoclay production. Journal of Science & Research (Civil & Environmental Engineering) (AJSR – CEE), Summer. 2013;**45**(1):11-13

[26] Charhouf I, Bennamara A, Abourriche A, Berrada M. Characterization of chitosan and fabrication of chitosan hydrogels matrices for biomedical applications. MATEC Web of Conferences 5. 2013;**04030**. DOI: 10.1051/matecconf/20130504030

[27] Standard Test Method for Tensile Properties of Thin Plastic Sheeting, Annual Book of ASTM Standards. Current edition approved April 10, 2002

[28] ASTM D882 published on June 2002, originally published as D 882-46 T. and Last previous edition is D 882-01

[29] Cheng LH, Karim AA, Seow CC. Effects of water-glycerol and water-sorbitol interactions on the physical properties of konjac glucomannan films. Journal of Food Science. March 2006;**71**(2). DOI: 10.1111/j.1365-2621.2006.tb08898.x

[30] Cuq B, Gontard N, Cuq J, Guilbert S. Selected functional properties of fish myofibrillar protein-based films as affected by hydrophilic plasticizers. Journal of Agricultural and Food Chemistry. 1997;**45**(3):622-626

[31] Karbowiak T, Hervet H, Léger L, Champion D, Debeaufort F, Voiley A. Effect of plasticizers (water and glycerol) on the diffusion of a small molecule in iota-carrageenan biopolymer films for edible coating application. Biomacromolecules. 2006;**7**(6):2011-2019

[32] Kristo E, Biliaderis CG. Water sorption and thermo-mechanical properties of water/sorbitol-plasticized composite biopolymer films: caseinate-pullulan bilayers and blends. Food Hydrocolloids. 2006;**20**(7):1057-1071

[33] Charhouf I, Bennamara A, Abourriche A, Chenite A, Zhu J, Berradae M. Characterization of a dialdehyde chitosan generated by periodate oxidation. International Journal of Sciences: Basic and Applied Research (IJSBAR). 2014;**16**(2):336-348

[34] Bilia AR, Guccione C, Isacchi B, Righeschi C, Firenzuoli F, Bergonzi MC. Essential oils loaded in nanosystems: a developing strategy for a successful therapeutic approach. Evidence-based Complementary and Alternative Medicine. 2014;**2014**:651593. DOI: 10.1155/2014/651593

[35] Wang L, Wang A. Adsorption characteristics of congo red onto the chitosan/montmorillonite nanocomposite. Journal of Hazardous Materials. 2007;**147**:979-985

[36] Paluszkiewicz C, Stodolak E, Hasik M, Blazewicz M. FT-IR study of montmorillonite–chitosan nanocomposite materials. Spectrochimica Acta Part A: Molecular and Biomolecular Spectroscopy. 2004;**79**:784-788

[37] Tan W, Zhang Y, Szeto Y, Liao L. A novel method to prepare chitosan/montmorillonite nanocomposites in the presence of hydroxy-aluminum oligomeric cations. Journal of Computer Science and Technology. 2008;**68**:2917-2921

[38] Darder M, Colilla M, Ruiz-Hitzky E. Chitosan-clay nanocomposites: application as. 500 electrochemical sensors. Journal Appl Clay Science. 2005;**28**:199-208

[39] Han Y, Lee SH, Choi KH, Park I. Preparation and characterization of chitosan–clay nanocomposites with antimicrobial activity. Journal of Physics and Chemistry of Solids. 2010;**71**: 464-467

[40] Laaraibi A, Charhouf I, Bennamara A, Abourriche A, Berrada M. Berrada. Valorization of marine wastes in a preserving film based on chitosan for food applications. Journal of Materials and Environmental Science. 2015;**6**(12):3511-3516